2014 IEEE International Conference on Robotics & Automation (ICRA)
Hong Kong Convention and Exhibition Center
May 31 - June 7, 2014. Hong Kong, China

Analysis of the Inverse Kinematics Problem for 3-DOF Axis-Symmetric Parallel Manipulators with Parasitic Motion

Mats Isaksson, Anders Eriksson and Saeid Nahavandi

Abstract— **Determining an analytical solution to the inverse kinematics problem for a parallel manipulator is typically a straightforward problem. However, lower mobility parallel manipulators with 2-5 degrees of freedom (DOFs) often suffer from an unwanted parasitic motion in one or more DOFs. For such manipulators, the inverse kinematics problem can be significantly more difficult. This paper contains an analysis of the inverse kinematics problem for a class of 3-DOF parallel manipulators with axis-symmetric arm systems. All manipulators in the studied class exhibit parasitic motion in one DOF. For manipulators in the studied class, the general solution to the inverse kinematics problem is reduced to solving a univariate equation, while analytical solutions are presented for several important special cases.**

I. INTRODUCTION

The field of kinematics is the study of motion without considering the forces that cause the motion. Simply put, the inverse kinematics (IK) problem means finding the actuated joint angles of a manipulator, knowing the position and orientation of its end-effector (EEF). For an industrial robot, the main use of the IK is to calculate the joint angles corresponding to a programmed path (positions and orientations) of the EEF. In addition to that, the derived expressions are useful for kinematic analysis of a manipulator, including studies of its isotropy and stiffness.

The section of the workspace where solutions to the IK exist is called the *reachable workspace*. The reachable workspace is limited by the arm lengths of the manipulator, joint limitations and collisions. If a solution does exist, it may not be unique. The IK could have multiple or even infinite solutions. The parallel manipulators (PMs) studied here are typically designed so that only one solution to the IK is valid. However, manipulators of the investigated type could be designed with the possibility of utilising multiple IK solutions. In [1], this possibility is explored for a 6-DOF variant of the manipulators studied here.

It is often loosely stated that the IK problem is complex for a serial manipulator (SM) whereas straightforward for a PM. However, while this is often the case, several exceptions exist. First of all, the IK for an SM does not have to be complex. Consider for example a serial 6-DOF mechanism whose base is attached to a 2-DOF joint with the same functionality as a universal joint, except that both joint axes are actuated. Assume this joint is connected to an actuated telescopic link, which in turn is connected to a manipulated platform via a 3-DOF joint with three concurrent and perpendicular joint axes that are all actuated (kinematically equivalent to a spherical joint). If the tool centre point (TCP) is assumed to be in the joint axes intersection point of the 3-DOF joint, the IK of this decoupled mechanism is straightforward with only one possible solution. However, for a typical 6-DOF serial industrial robot, the manipulator DOFs are not decoupled, leading to a more complex IK problem. For such manipulators, the solution for each joint is typically dependent on the solution of other joints in the kinematic chain and can not be determined independently. Furthermore, such mechanisms typically feature multiple IK solutions.

Similarly, the IK for a parallel robot is not always straightforward. As most definitions of a parallel robot allows for more than one actuated joint per kinematic chain, a 6-DOF parallel robot may have as few as two kinematic chains and one of these chains may include five actuated joints. In this case, the complexity of the IK problem is similar to that of a 5-DOF SM and hence more intricate. A redundant parallel robot could be composed of two 6-DOF SMs connected at the EEF, in which case the complexity of the IK problem is more than double that of a 6-DOF SM.

For a *fully parallel manipulator*, each kinematic chain only features one actuated joint. Hence, each joint coordinate can typically be calculated independently of the other joints. Deriving an analytical solution to the IK for such manipulators is usually uncomplicated. However, as will be demonstrated in this paper, finding analytical solutions to the IK for fully parallel manipulators may also be intricate. This is often the case for lower mobility PMs, as mechanisms of this type commonly suffer from an unwanted coupled motion of the EEF. Such motion was named parasitic motion in [2]. Due to the parasitic motion, the position and orientation of the EEF is not completely known. Even though the unknown EEF coordinates are not required to be determined explicitly, solving the IK problem for mechanisms with parasitic motion typically involves calculating both the unknown EEF coordinates and the coordinates of the actuated joints.

This paper provides a study of the IK problem for a class of 3-DOF PMs with axis-symmetric arm systems. The actuated upper arms of the investigated axis-symmetric PMs have a common axis of rotation, leading to equal manipulator properties in all radial half planes defined by this common axis. All manipulators in the investigated class suffer from parasitic motion of the EEF in one DOF, which complicates the IK problem.

M. Isaksson and S. Nahavandi are with the Centre for Intelligent Systems Research (CISR), Deakin University, Australia. E-mail: mats.isaksson@gmail.com, saeid.nahavandi@deakin.edu.au. A. Eriksson is with the School of Computer Science, University of Adelaide, Australia. E-mail: anders.eriksson@adelaide.edu.au.

978-1-4799-3685-4/14/$31.00 ©2014 IEEE

The studied manipulator variants are introduced in Section II. This class of manipulators includes all variants of the SCARA-Tau robot [3]. The IK of the original SCARA-Tau prototype was first presented in [4]. In [5], an alternative derivation of the IK for this manipulator was proposed and a solution for a SCARA-Tau variant with triangular link configuration, proposed in [6], was introduced. However, both [4, 5] only consider the case when the TCP is equal to the position of a platform joint. Additional variants of the SCARA-Tau have been proposed in [7]. This paper presents solutions to the IK problem for general SCARA-Tau variants with arbitrary choice of TCP. Additionally, the IK problem is solved for all variants of the Symmetric SCARA manipulator proposed in [7] and for another similar mechanism introduced in [8].

A table of abbreviations used throughout the paper is provided in Table I.

II. 3-DOF AXIS-SYMMETRIC MANIPULATORS

Figure 1 shows six variants of the 3-DOF axis-symmetric PMs studied in this paper. All the investigated manipulators comprise a cylindrical base column and an axis-symmetric arm system. The arm system is composed of three actuated upper arms with a common axis of rotation, a manipulated platform, and six 5-DOF or 6-DOF lower arm linkages (LALs) connecting the upper arms and the manipulated platform. The LALs are constructed by a fixed-length link with a 3-DOF spherical joint on one end and either another one of these joints or a 2-DOF universal joint on the other end. All actuators are mounted on the fixed base column. As the links in such LALs are only susceptible to axial forces, they can have a light-weight construction, for example using carbon fibre. The axis-symmetric arm system leads to an extensive positional workspace while the possibility for infinite rotation of the arm system means the manipulators can always use the shortest path between two programmed positions.

For the studied class of manipulators, two pairs of LALs are mounted to form parallelograms in separate planes parallel to the common axis of rotation of the upper arms. Such parallelograms are in the future text referred to as *vertical parallelograms*, even if that is only true if the common axis of rotation of the upper arms is vertical. The two vertical parallelograms keep two rotational DOFs of the manipulated platform constant in the entire workspace. The only possible platform rotation is around an axis parallel to the common axis of rotation of the upper arms. Ideally, this platform rotation should remain constant during vertical and radial motions of the manipulated platform. However, this is not the case, meaning these manipulators suffer from a parasitic rotation of the manipulated platform. Parasitic rotation is further discussed in Section V-A.

TABLE I

TABLE OF ABBREVIATIONS

IK	Inverse kinematics
PM	Parallel manipulator
SM	Serial manipulator
TCP	Tool centre point
EEF	End-effector
LAL	Lower arm linkage

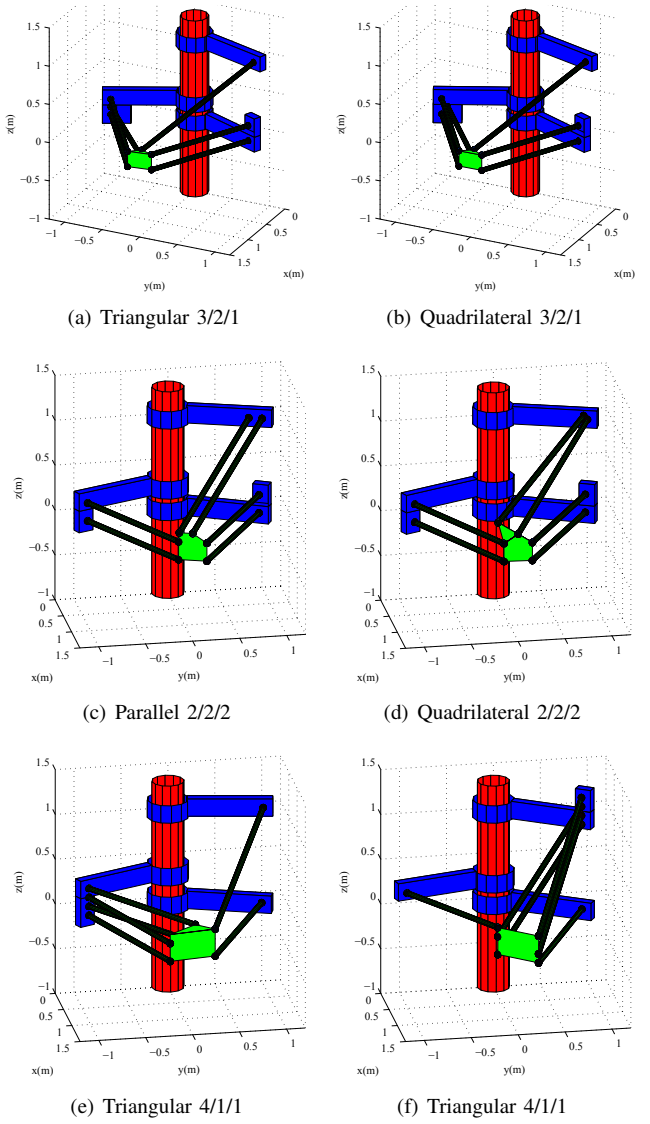

(a) Triangular 3/2/1 (b) Quadrilateral 3/2/1

(c) Parallel 2/2/2 (d) Quadrilateral 2/2/2

(e) Triangular 4/1/1 (f) Triangular 4/1/1

Fig. 1. 3-DOF axis-symmetric manipulators with different link clustering. For the manipulator in (a), all upper arm joints in the cluster of three links are collinear while this is not the case in for the manipulator in (b). For the manipulators in (e) and (f), the upper arm joints in the cluster of four links are collinear and the vertical distances between neighbouring joints on the upper arm are the same as the vertical distances between the corresponding joints on the manipulated platform.

The manipulators in Fig. 1(a) and (b) are variants of the SCARA-Tau manipulator [3]. For the original SCARA-Tau manipulator, the LALs in the cluster of three are parallel. The SCARA-Tau variants in Fig. 1(a) and (b) were introduced in [6] and [7], respectively. They are identical to the original SCARA-Tau manipulator except for a different position and orientation of the LAL in the cluster of three that is not part of the vertical parallelogram. Different arrangements of this LAL may be used to minimise the parasitic rotation of the platform or to maximise the manipulator isotropy [7, 8]. The names *Triangular* and *Quadrilateral* are based on the shapes

formed by a projection of the cluster of three links in the x-y plane. Other variants of the SCARA-Tau manipulator were proposed in [7, 8].

The manipulators in Fig. 1(c) and (d) are two variants of the Symmetric SCARA mechanism introduced in [7]. One advantage of the 2/2/2 clustering compared to the 3/2/1 clustering of the SCARA-Tau is a more equal force distribution in the LALs. Both the Symmetric SCARA and the SCARA-Tau may also be designed with a collinear arrangement of the platform joints of the two vertical parallelograms [7].

The possibility of utilising a 4/1/1 clustering of the LALs were discussed in [8]. The manipulators in Fig. 1(e) and (f) are two examples of such manipulators. The 4/1/1 clustering typically leads to a small angle between the two planes containing the vertical parallelograms and the stiffness for such variants must be carefully evaluated. Possibilities to maximise this stiffness (e.g. by using a wider manipulated platform) are discussed in [8]. Even though the 4/1/1 configurations and the 3/2/1 configurations have very different manipulator properties, their IK solutions are equivalent. Hence, the IK solutions for the 4/1/1 mechanisms are not explicitly discussed in this paper.

For all the illustrated manipulator variants, the linkages in both parallelograms form equal angles with a horizontal plane; however, this is not a necessary condition and other arrangements are also possible [8].

III. NOTATION

A. Bodies

The bodies and kinematic parameters of a 3/2/1 variant of the studied mechanisms are shown in Fig. 2. For a 2/2/2 configuration, the notations U_{13}, P_{13}, L_{13}, a_{13}, l_{13}, h_{13} are replaced by U_{32}, P_{32}, L_{32}, a_{32}, l_{32}, h_{32}.

The cylindrical base column B is connected to several upper arms A_i via 1-DOF revolving joints R_i. These joints are actuated with a common axis of rotation in the centre of the base column B. The upper arms A_i are not necessarily horizontal, which makes it possible to minimise the height of the base cylinder. The index i is determined by the ordering of the upper arms, where $i = 1$ for the upper arm containing the lowest upper arm joint. If the lowest upper arm joints of two upper arms are mounted at equal height, the upper arm with a 'right-arm' solution is given the lower value of i.

Each upper arm A_i is connected via a joint U_{ij} to a lower arm link L_{ij}. The index j is used to differ between joints on the same upper arm. The index is determined by the height of the upper arm joints and the lowest joint on each upper arm is assigned $j = 1$. If two joints on one upper arm are mounted at the same height, the lowest value of j is assigned to the joint with the largest perpendicular distance to the common axis of rotation.

The notation U refers to the location of the joint on the upper arm and does not describe the type of joint. The upper arm joints U_{ij} are typically spherical joints or joints kinematically equivalent to spherical joints, allowing rotation around three concurrent joint axes. However, they could also be 2-DOF universal joints, in which case the corresponding

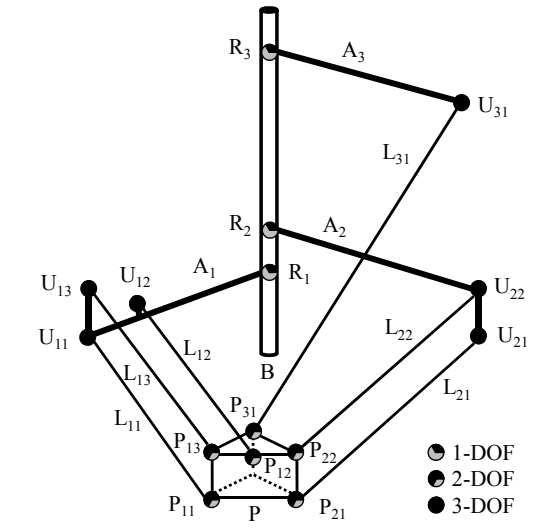

(a) Bodies and joints (3/2/1)

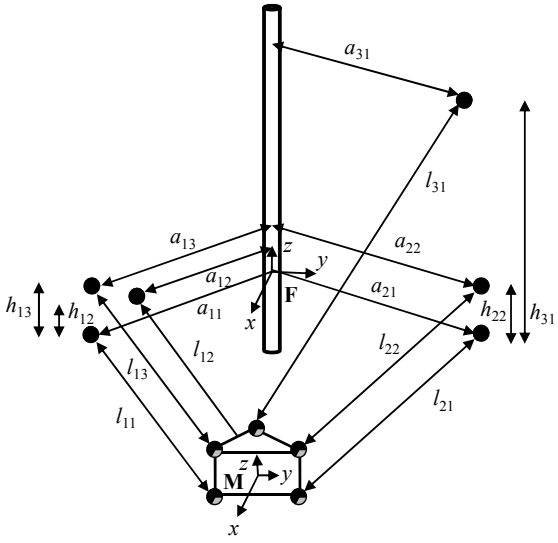

(b) Kinematic parameters (3/2/1)

Fig. 2. Bodies, joints, defined coordinate systems and kinematic parameters of a SCARA-Tau manipulator (3/2/1).

joints on the manipulated platform would be 3-DOF spherical joints.

Each lower arm link L_{ij} is connected via a joint P_{ij} to a manipulated platform P. The notation P refers to the location of the joint on the manipulated platform and not to the type of joint. These joints are typically 2-DOF universal joints. However, they could also be spherical joints or joints kinematically equivalent to spherical joints. In order to simplify the kinematics, all 2-DOF and 3-DOF joints are assumed to have concurrent axes of rotation.

The studied mechanisms may utilise joints which provide infinite rotation around the lower arm link axis and +-90° around both the other axes. Examples of such joints are provided in [9], which also shows how the joint limitations for such joints may be implemented.

B. Joint Positions on the Upper Arms

The kinematic parameters of the studied manipulators are indicated in Fig. 2(b). A fixed coordinate system **F** is defined with its z-axis being the common rotation axis of the joints R_i. The x-axis and y-axis of the coordinate system **F** are defined to be in the plane perpendicular to the z-axis passing through the common intersection point of the joint axes of U_{11}. Because the manipulator is axis-symmetric, the x-axis is defined to be an arbitrary direction in this plane while the y-axis is defined according to the right hand rule.

The angles q_i of the upper arms A_i are measured from the x-axis of **F** according to the right-hand rule. Each upper arm joint U_{ij} is mounted at a perpendicular distance a_{ij} from the z-axis of **F** with a z-coordinate h_{ij}. The value of h_{11} is by definition zero. The position of each joint U_{ij} is expressed in **F** as

$$^{\mathbf{F}}\mathbf{u}_{ij} = [u_{ijx}, u_{ijy}, u_{ijz}]^{\mathrm{T}} = [a_{ij}\cos(q_i), a_{ij}\sin(q_i), h_{ij}]^{\mathrm{T}}. \quad (1)$$

C. Joint Positions on the Manipulated Platform

A tool coordinate system **M** is defined on the manipulated platform P with its origin in the TCP. The position of each joint P_{ij} on the manipulated platform P is expressed in **M** as

$$^{\mathbf{M}}\mathbf{p}_{ij} = [^{\mathbf{M}}p_{ijx}, ^{\mathbf{M}}p_{ijy}, ^{\mathbf{M}}p_{ijz}]^{\mathrm{T}}. \quad (2)$$

The distance between a joint U_{ij} on an upper arm and the corresponding joint P_{ij} on the manipulated platform is l_{ij}. This is the kinematic length of the link L_{ij}.

The position of the TCP in the fixed coordinate system, **F**, is given by the three translations x, y, z. The platform orientation remains constant except for a position dependent yaw rotation ϕ around an axis parallel to the common axis of rotation of the three upper arms. The platform joint positions in the fixed coordinate system are

$$^{\mathbf{F}}\mathbf{p}_{ij} = [p_{ijx}, p_{ijy}, p_{ijz}]^{\mathrm{T}} = {}^{\mathbf{F}}\mathbf{o}_{\mathbf{M}} + {}^{\mathbf{F}}R_{\mathbf{M}}{}^{\mathbf{M}}\mathbf{p}_{ij}, \quad (3)$$

where

$$^{\mathbf{F}}\mathbf{o}_{\mathbf{M}} = [x, y, z]^{\mathrm{T}}, \quad (4)$$

$$^{\mathbf{F}}R_{\mathbf{M}} = R_{\mathrm{z}}(\phi) = \begin{pmatrix} \cos(\phi) & -\sin(\phi) & 0 \\ \sin(\phi) & \cos(\phi) & 0 \\ 0 & 0 & 1 \end{pmatrix}. \quad (5)$$

IV. SUB-PROBLEM OF THE INVERSE KINEMATICS

A sub-problem of the IK problem is determining the joint angle q_i of an upper arm A_i, connected via a lower arm link L_{ij} to a platform joint P_{ij}, if the position of the joint P_{ij} in the fixed coordinate system **F** is known. This problem is relatively straightforward and has been presented previously; however, for completeness it is included here. For manipulators without parasitic motion, the position and orientation of the manipulated platform is completely known and the position of all joints P_{ij} are immediately found from (3), which means this sub-problem comprises the complete IK problem.

The joint angles can be determined using a *geometric approach* or an *algebraic approach*. The algebraic approach involves defining length equations for the constant distances between the passive links in a mechanism and thereafter solving the derived non-linear equation system without further regard to the geometry of the manipulator. While this approach often seems more systematic, sometimes the equations end up unnecessarily complex and the solution often fails to provide physical insight into a mechanism. A geometric approach uses understanding of the geometric structure of a manipulator to derive equations, for example, noting that certain angles or distances remain constant or utilising trigonometric functions, such as the law of cosines. This approach is often less systematic; however, it often leads to more insight into a mechanism. Both approaches are demonstrated here. In general, they involve the same computational complexity and it is not unusual to end up solving the same equations.

A. Algebraic Approach

If the positions of the platform joints are known, the joint angles may be determined algebraically from the length equations of the lower arm links L_{ij}. Squaring those equations gives

$$|^{\mathbf{F}}\mathbf{p}_{ij} - {}^{\mathbf{F}}\mathbf{u}_{ij}|^2 - l_{ij}^2 = 0. \quad (6)$$

Using (1) and (3) to expand the equations (6) leads to

$$c_{ija} + c_{ijb}\sin(q_i) + c_{ijc}\cos(q_i) = 0, \quad (7)$$

where parameters c_{ijk} have been introduced according to

$$\begin{aligned} c_{ija} &= p_{ijx}^2 + p_{ijy}^2 + (p_{ijz} - h_{ij})^2 + a_{ij}^2 - l_{ij}^2, \\ c_{ijb} &= -2a_{ij}p_{ijy}, \\ c_{ijc} &= -2a_{ij}p_{ijx}. \end{aligned} \quad (8)$$

If $c_{ija} \neq c_{ijc}$, each equation (7) has two solutions. One solution $q_{i\mathrm{R}}$ corresponds to a right upper arm and one solution $q_{i\mathrm{L}}$ corresponds to a left upper arm:

$$\begin{aligned} q_{i\mathrm{R}} &= -2\arctan\left(\frac{c_{ijb} + \sqrt{-c_{ija}^2 + c_{ijb}^2 + c_{ijc}^2}}{c_{ija} - c_{ijc}}\right), \\ q_{i\mathrm{L}} &= -2\arctan\left(\frac{c_{ijb} - \sqrt{-c_{ija}^2 + c_{ijb}^2 + c_{ijc}^2}}{c_{ija} - c_{ijc}}\right). \end{aligned} \quad (9)$$

The positions of a right and a left upper arms can be seen in Fig. 3. For the special case of $c_{ija} = c_{ijc}$, one of the two possible angles is always 180°, while the other angle is either $-\arcsin\left(\frac{2c_{ija}c_{ijb}}{c_{ija}^2+c_{ijb}^2}\right)$ or $180^\circ + \arcsin\left(\frac{2c_{ija}c_{ijb}}{c_{ija}^2+c_{ijb}^2}\right)$, depending on which of these solutions that fulfil (7).

B. Geometric Approach

The solution in (9) is compact but does not provide much physical insight into the mechanism. Determining the actuated joint angles geometrically leads to a somewhat different solution and an increased understanding of the mechanism.

Figure 3 shows the two possible upper arm angles, q_i, knowing the x and y coordinates of one platform joint P_{ij},

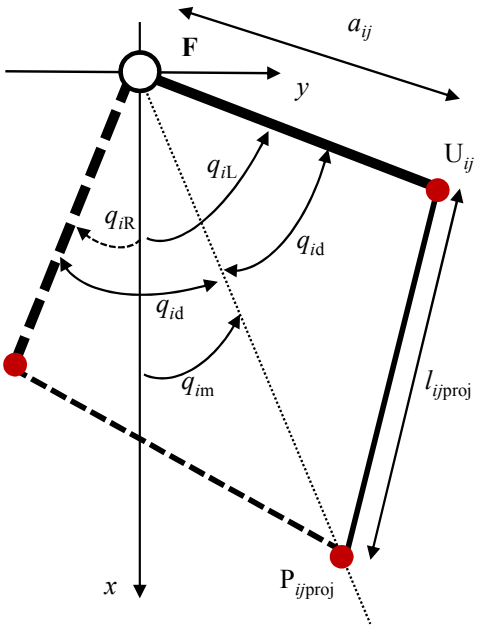

Fig. 3. The two possible joint angles q_{iR} and q_{iL} of an upper arm A_i for a known position of the joint P_{ij}.

together with the upper arm length a_{ij} and the length l_{ijproj}. The length l_{ijproj} is the length of L_{ij} projected in the xy-plane. It is determined from Pythagoras' theorem:

$$l_{ijproj} = \sqrt{l_{ij}^2 - (p_{ijz} - h_{ij})^2}. \tag{10}$$

As can be seen from Fig. 3, the two possible solutions are:

$$\begin{aligned} q_{iR} &= q_{im} - q_{id}, \\ q_{iL} &= q_{im} + q_{id}, \end{aligned} \tag{11}$$

where

$$\begin{aligned} q_{im} &= \arctan2\left(p_{ijy}, p_{ijx}\right), \\ q_{id} &= \arccos\left(\frac{p_{ijx}^2 + p_{ijy}^2 + a_{ij}^2 - l_{ijproj}^2}{2a_{ij}\sqrt{p_{ijx}^2 + p_{ijy}^2}}\right). \end{aligned} \tag{12}$$

The first term, q_{im}, is calculated using only p_{ijx} and p_{ijy}, given by (3). The case when both p_{ijx} and p_{ijy} are zero lacks solutions due to collisions. The second term, q_{id}, is obtained from p_{ijx}, p_{ijy} and the manipulator arm lengths using the law of cosines. Two solutions always exist on both sides of q_{im}, except when the upper arm and the lower arm link are collinear, in which case q_{id} becomes zero. The two solutions separate different working modes of the mechanism. A configuration with only one solution signifies a Type 1 or Type 3 singularity [10].

V. COMPLETE INVERSE KINEMATICS

A. Parasitic Motion

Calculating analytical solutions to the IK for a lower mobility axis-symmetric PM exhibiting parasitic motion can be an intricate problem. If the six LALs of the manipulators in Fig. 1 were connected to arbitrary positions on the manipulated platform, actuation of the three upper arms could lead to 6-DOF motion of the platform. For such a manipulator, the motion in three DOFs can be controlled whereas the motion in the other three DOFs is a coupled parasitic motion. In this case, the IK must be determined when only three of the six coordinates describing the platform position and orientation are explicitly known, which is an exceedingly difficult problem. However, a manipulator exhibiting parasitic motion in three DOFs would also be of limited practical use. Axis-symmetric PMs including two vertical parallelograms, as in Fig. 1, exhibit parasitic motion in only one DOF. The variation of the yaw angle during radial and vertical motion of the TCP is considered parasitic and should ideally remain constant. The yaw angle ϕ may be expressed as

$$\phi(x,y,z) = \arctan2(y,x) + \phi_m + \phi_p(x,y,z), \tag{13}$$

where ϕ_m is the average of $\phi(x,y,z)$ calculated over the plane where $y = 0$. Both ϕ_m and the parasitic yaw angle $\phi_p(x,y,z)$ depend on the manipulator architecture and the choice of TCP on the manipulated platform. However, the term ϕ_m can always be eliminated by modifying the definition of the coordinate system $\mathbf{M}$ relative to the manipulated platform. If the orientation of $\mathbf{M}$ is selected depending on the platform normal, modifying $\mathbf{M}$ corresponds to adding a constant rotation offset to the platform.

A manipulator has the potential to be free of parasitic yaw rotation if it is possible to select a TCP on the manipulated platform such that the term $\phi_p(x,y,z)$ is zero in the entire workspace. For the 3-DOF manipulators in Fig. 1 this is not possible, which means finding analytical solutions to the IK for these mechanisms is a difficult problem.

Solving the IK for the 3-DOF PMs in Fig. 1 means determining three joint angles when only the position of the EEF (x, y, z) is explicitly known. Two tilt angles of the platform are implicitly known, as they remain constant in the entire workspace. Due to the parasitic motion, the yaw angle (ϕ) is unknown.

Preferably, the IK should be solvable for an arbitrary mounting of the EEF on the manipulated platform. However, it is sometimes possible to find an analytical solution for a particular choice of TCP, even if an analytical solution for an arbitrary TCP cannot be determined. As will be shown, for the studied manipulators the solution is simplified if the TCP is assumed to have the same horizontal position as one of the joints on the manipulated platform. Even if finding an analytical solution for an arbitrary TCP is preferable, finding an analytical solution for a non-arbitrary TCP may still be useful for kinematic studies of the manipulator. Also in this case, the derived expressions completely describe the motion of the manipulated platform and can be used to calculate Jacobians, singular values, condition numbers and for studying the parasitic motion of the manipulator.

B. General Case

For both the algebraic solution (9) and the geometric solution (11), the upper arm angles q_{iL} and q_{iR} are determined

from the position of one platform joint P_{ij} in the fixed coordinate system **F**. This position (p_{ijx}, p_{ijy}, p_{ijz}) is in turn dependent on ϕ according to (4).

In this section we instead use the notation $q_{ij\mathrm{R}}$ and $q_{ij\mathrm{L}}$ for the upper arm angles determined from one platform joint P_{ij}. Let $q_{ik\mathrm{R}}$ and $q_{ik\mathrm{L}}$ be different calculations of the same upper arm angles based on another platform joint P_{ik} connected by a LAL L_{ik} to the same upper arm, where L_{ik} must have a different horizontal projection than L_{ij}. As both calculations of the upper arm angles should give the same result, it follows that $q_{ij\mathrm{R}} = q_{ik\mathrm{R}}$ and $q_{ij\mathrm{L}} = q_{ik\mathrm{L}}$.

For the Symmetric SCARA variants in Fig. 1(c) and (d), the two links must be $L_{ij} = L_{31}$ and $L_{ik} = L_{32}$. For the illustrated variants the correct solution is $q_3 = q_{3\mathrm{L}}$. Hence, the yaw angle of the illustrated Symmetric SCARA manipulators may be determined by solving:

$$q_{31\mathrm{L}}(\phi) - q_{32\mathrm{L}}(\phi) = 0. \tag{14}$$

For the SCARA-Tau variants in Fig. 1(a) and (b), the links used are selected to be $L_{ij} = L_{11}$ and $L_{ik} = L_{12}$ according to Fig. 2. The correct solution for these variants is $q_1 = q_{1\mathrm{R}}$. Hence, the corresponding equation for the SCARA-Tau manipulator is

$$q_{11\mathrm{R}}(\phi) - q_{12\mathrm{R}}(\phi) = 0. \tag{15}$$

The only unknown variable in (14) and (15) is the yaw angle ϕ. These equations have two solutions, where only one is physically possible due to collisions and joint limitations. Typically, the studied manipulators are designed to minimize ϕ_{m} and $\phi_{\mathrm{p}}(x,y,z)$ in (13), meaning $\arctan2(y,x)$ is a good initial value to numerically find the valid solution. After determining ϕ from (14) or (15), q_1, q_2 and q_3 can be calculated using (9) or (11).

The equations (14) and (15) may be expanded using either the algebraic IK solution (9) or the geometric IK solution (11).

C. Non-arbitrary TCP

If the TCP (origin of **M**) is selected to have the same horizontal position as a joint P_{ij}, then p_{ijx}, p_{ijy} and p_{ijz} in (8) are equal to x, y, and $z + {}^{\mathbf{M}}p_{ijz}$, respectively, in which case q_i is immediately determined from (9). Thereafter, a length equation for a second link L_{ik} on the same upper arm A_i can be reformulated as

$$d_{ik\mathrm{a}}(q_i) + d_{ik\mathrm{b}}(q_i)\sin(\phi) + d_{ik\mathrm{c}}(q_i)\cos(\phi) = 0, \tag{16}$$

with variables

$$\begin{aligned}
d_{ik\mathrm{a}}(q_i) &= x^2 + y^2 + z^2 + a_{ik}^2 - l_{ik}^2 + {}^{\mathbf{M}}p_{ik\mathrm{x}}^2 + {}^{\mathbf{M}}p_{ik\mathrm{y}}^2 \\
&\quad + ({}^{\mathbf{M}}p_{ik\mathrm{z}} - h_{ik})^2 + 2({}^{\mathbf{M}}p_{ik\mathrm{z}} - h_{ik})z \\
&\quad - 2a_{ik}y\sin(q_i) - 2a_{ik}x\cos(q_i), \\
d_{ik\mathrm{b}}(q_i) &= -2{}^{\mathbf{M}}p_{ik\mathrm{y}}x + 2{}^{\mathbf{M}}p_{ik\mathrm{x}}y \\
&\quad - 2a_{ik}{}^{\mathbf{M}}p_{ik\mathrm{x}}\sin(q_i) + 2a_{ik}{}^{\mathbf{M}}p_{ik\mathrm{y}}\cos(q_i), \\
d_{ik\mathrm{c}}(q_i) &= 2{}^{\mathbf{M}}p_{ik\mathrm{x}}x + 2{}^{\mathbf{M}}p_{ik\mathrm{y}}y \\
&\quad - 2a_{ik}{}^{\mathbf{M}}p_{ik\mathrm{y}}\sin(q_i) - 2a_{ik}{}^{\mathbf{M}}p_{ik\mathrm{x}}\cos(q_i).
\end{aligned} \tag{17}$$

This equation is of the same type as (7) and can be solved the same way. After ϕ has been calculated, the two remaining upper arm angles can be determined using (9) or (11).

The presented solution for a non-arbitrary TCP is valid for all Symmetric SCARA variants if the TCP has the same horizontal position as P_{m1} or P_{m2}, where m is the index of the upper arm not including a vertical parallelogram. Similarly, the solution is valid for all SCARA-Tau variants if the TCP has the same horizontal position as P_{m1}, P_{m2} or P_{m3}, where m is the index of the upper arm including three LALs.

D. Parallel and Triangular Link Configurations

For the Parallel Symmetric SCARA in Fig. 1(c) and the corresponding SCARA-Tau variant (the original SCARA-Tau), analytical solutions are possible also for an arbitrary TCP (origin of **M**). This is also the case for the Triangular SCARA-Tau in Fig. 1(a) and the corresponding triangular configuration of a Symmetric SCARA manipulator.

Figure 4 shows projections of the parallel and triangular SCARA-Tau manipulators in a horizontal plane. Only two of the upper arms and the LALs connected to these arms are included. For the SCARA-Tau manipulator, one of the upper arms must be the one holding the cluster of three LALs while the other arm must be the one holding the cluster of two LALs. The notation in Fig. 4 and the solution presented here are for two SCARA-Tau variants; however, the solution is equivalent for the corresponding Symmetric SCARA variants. For the corresponding projections of the Symmetric SCARA manipulator, one upper arm must be the one not including a vertical parallelogram and the other upper arm must have a different arm solution ($q_{i\mathrm{L}}$ or $q_{i\mathrm{R}}$) when compared to this arm.

The length $l_{11\mathrm{proj}}$ in Fig. 4(a) is the length of L_{11}'s projection in the xy-plane given by (10). The required heights p_{ijz} of the platform joint positions in the fixed coordinate system **F** are immediately determined from the z-coordinate ($p_{ijz} = z + {}^{\mathbf{M}}p_{ijz}$). The angle ϕ_0 is constant and known.

The IK is calculated by applying Pythagoras' theorem in the two right-angled triangles $C_1C_2C_3$ and $\mathbf{F}C_2\mathbf{M}$ shown in Fig. 4(a). The distances c_1 and c_2 are constant and known. The variable s_2 is always positive, while the variable s_1 can be both negative and positive. Pythagoras' theorem gives

$$\begin{aligned}
l_{11\mathrm{proj}}^2 &= s_1^2 + s_2^2, \\
x^2 + y^2 &= (a_{12} + c_1 + s_1)^2 + (c_2 + s_2)^2.
\end{aligned} \tag{18}$$

The condition $s_2 > 0$ leads to a unique solution of (18). After s_1 has been determined from (18), the angle q_1 is calculated according to

$$q_1 = \arctan2\,(y,x) - \arccos\left(\frac{a_{12} + c_1 + s_1}{\sqrt{x^2 + y^2}}\right). \tag{19}$$

The yaw angle ϕ is determined from q_1 and the constant rotational offset ϕ_0 according to

$$\phi = q_1 + \frac{\pi}{2} - \phi_0. \tag{20}$$

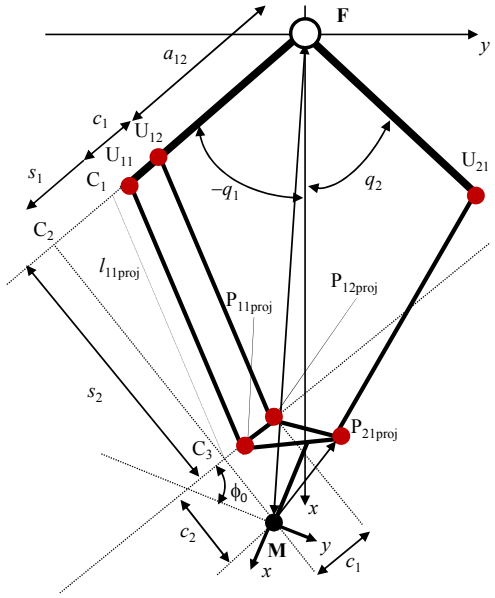

(a) Parallel SCARA-Tau

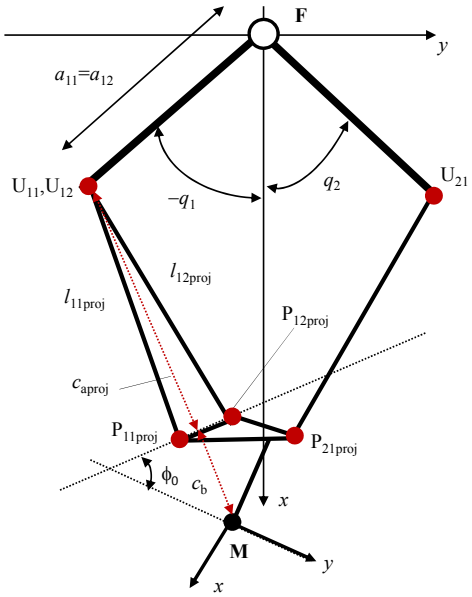

(b) Triangular SCARA-Tau

Fig. 4. Horizontal projections of two variants of the SCARA-Tau manipulator. Only two of the three kinematic chains have been included.

After ϕ has been calculated, it is straightforward to determine the two remaining upper arm angles using (9) or (11).

The IK problem for the Triangular SCARA-Tau in Fig. 1(a) and the corresponding Triangular Symmetric SCARA manipulator can also be solved analytically for an arbitrary choice of TCP. Fig. 4(b) show a projection of the Triangular SCARA-Tau in the xy-plane. Only two of the upper arms and the LALs connected to these arms are included. The distance c_b is constant and known while the distance c_aproj is the projection of a constant and known length in the xy-plane. The angle ϕ_0 is constant and known. The position of U_{11} can be determined from the intersection of one circle with centre point in the origin of **M** and radius $c_\mathrm{aproj}+c_\mathrm{b}$ and another circle with centre point in the origin of the coordinate system **F** and radius a_{11} (equivalent to solving the length equations for the constant distances a_{11} and $c_{1\mathrm{aproj}}+c_{1\mathrm{b}}$). This leads to two solution ${}^{\mathbf{F}}\mathbf{u}_{11}$. For the valid solution, the z-element in the vector product ${}^{\mathbf{F}}\mathbf{u}_{11}\times([\mathrm{x,y,0}]^\mathrm{T}$ is positive.

The length equations for the known distances $l_{11\mathrm{proj}}$ and $|{}^{\mathbf{M}}\mathbf{p}_{11\mathrm{proj}}|$ are used to determine the position of P_{11}, while the length equations for $l_{12\mathrm{proj}}$ and $|{}^{\mathbf{M}}\mathbf{p}_{12\mathrm{proj}}|$ are used to determine the position of P_{12}. The yaw angle ϕ can then be calculated according to $\phi=-\arctan2(p_{12\mathrm{x}}-p_{11\mathrm{x}},p_{12\mathrm{y}}-p_{11\mathrm{y}})-\phi_0$ while the position of P_{21} can be determined using (3). These calculations lead to multiple solutions; however, the valid solution may be selected by the conditions $|{}^{\mathbf{M}}\mathbf{p}_{11\mathrm{proj}}-{}^{\mathbf{M}}\mathbf{p}_{12\mathrm{proj}}|=|{}^{\mathbf{F}}\mathbf{p}_{11\mathrm{proj}}-{}^{\mathbf{F}}\mathbf{p}_{12\mathrm{proj}}|$ and $|{}^{\mathbf{M}}\mathbf{p}_{11\mathrm{proj}}-{}^{\mathbf{M}}\mathbf{p}_{21\mathrm{proj}}|=|{}^{\mathbf{F}}\mathbf{p}_{11\mathrm{proj}}-{}^{\mathbf{F}}\mathbf{p}_{21\mathrm{proj}}|$.

After ϕ has been calculated, it is straightforward to determine all three upper arm angles using (9) or (11).

VI. Verification

Figure 5 provides a verification of the derived equations. The IK is calculated for three of the manipulators in Fig. 1 during a radial motion of the TCP (origin of **M**). For all three manipulators, the TCP is selected to be in the centre of the manipulated platform between the four platform joints of the parallelograms. For all evaluated positions, the values of y and z are zero while the value of x has been varied. The minimum value of x is limited by collision between the lower arm links and the base column. The collisions have here been identified by visual inspection in the MATLAB models in Fig. 1; however, an automatic collision detection for manipulators of this type may be implemented according to the description in [9]. The maximum value of x is limited by the lengths of the upper arms and lower arm links.

For each of the three studied manipulators, the values of q_1, q_2, q_3 and ϕ have been calculated by one semi-numerical method and one analytical method. The applied analytical method differs between the three manipulators whereas the semi-numerical method used is the same in all three cases. The semi-numerical method involves determining ϕ by solving (14) or (15) using MATLAB's *fsolve* function and then calculating q_1, q_2 and q_3 using (9). The equations (14) and (15) were expanded by the geometric IK solution (11).

Figure 5(a) shows the results of the IK calculations for the Parallel Symmetric SCARA manipulator in Fig. 1(c). The analytical solution is calculated by applying the method described in relation to Fig. 4(a). The largest difference between corresponding angles calculated by the semi-numerical and the analytical methods in any evaluated position is 2×10^{-8} degrees.

Figure 5(b) shows the results of the IK calculations for the Quadrilateral Symmetric SCARA manipulator in Fig. 1(d). For this manipulator, the selected TCP has the same horizontal position as joint P_{31}, which means it is possible to apply the analytical method described in Section V-C. The largest

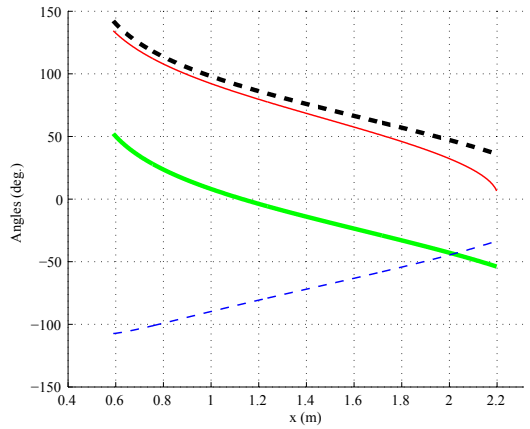

(a) Parallel Symmetric SCARA (2/2/2)

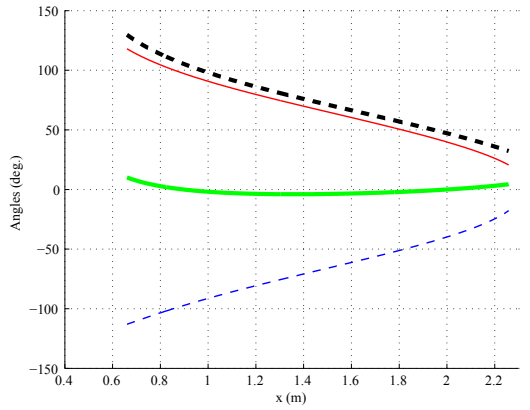

(b) Quadrilateral Symmetric SCARA (2/2/2)

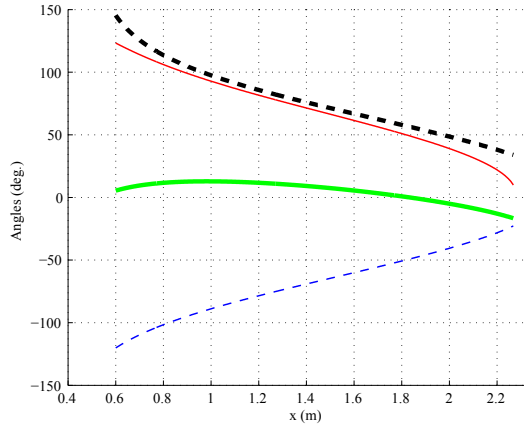

(c) Triangular SCARA-Tau (3/2/1)

Fig. 5. Verification of the derived equations for the manipulators in Fig. 1(c), (d) and (a). The yaw angle ϕ is plotted in thick solid green, q_1 in thin dashed blue, q_2 in thin solid red and q_3 in thick dashed black.

difference between corresponding angles calculated by the semi-numerical and the analytical methods in any evaluated position is 7×10^{-10} degrees.

Figure 5(c) shows the results of the IK calculations for the Triangular SCARA-Tau manipulator in Fig. 1(a). An analytical solution to the IK problem is calculated by applying the method described in relation to Fig. 4(b). The largest difference between corresponding angles calculated by the semi-numerical and the analytical methods in any evaluated position is 4×10^{-8} degrees.

As can be seen in Fig. 5, the size of the parasitic yaw angle variation is very different for the three manipulators with the largest variation for the Parallel Symmetric SCARA manipulator in Fig. 1(c). While the yaw angle variation may not be eliminated, the Quadrilateral variants minimises this variation [8]. The optimal quadrilateral shape depends on the length ratio between the lower arm links and the upper arms. If this ratio is large, the optimal quadrilateral shape is closer to a triangle, while for ratios closer to one, the optimal quadrilateral shape is closer to a parallelogram.

VII. Conclusion and Future Work

This paper analysed the IK problem for a class of 3-DOF axis-symmetric PMs. The manipulators in this class are composed of three actuated upper arms and six 5-DOF LALs, four of which are mounted to form two vertical parallelograms. All manipulators in this class exhibit an unwanted parasitic platform rotation in one DOF, which means the IK problem for these manipulators is intricate. It has been demonstrated that, in the general case, the IK problem can be reduced to solving one univariate equation numerically whereas analytical solutions have been presented for several important special cases.

As the IK will typically be used for real-time automatic control, valuable future work includes a comparison of the efficiency between the analytical and semi-numerical algorithms. A fully numerical algorithm should also be included as a benchmark.

References

[1] M. Isaksson and M. Watson, "Workspace Analysis of a Novel 6-DOF Parallel Manipulator with Coaxial Actuated Arms," *Journal of Mechanical Design*, vol. 135, no. 10, 104501, 2013.

[2] J. A. Carretero, R. P. Podhorodeski, M. A. Nahon, and C. M. Gosselin, "Kinematic Analysis and Optimization of a New Three Degree-of-Freedom Spatial Parallel Manipulator," *Journal of Mechanical Design*, vol. 122, no. 1, pp. 17–24, 2000.

[3] S. Kock, R. Oesterlein, and T. Brogårdh, "Industrial robot," WO Patent 03/066289 A1, Aug. 14, 2003.

[4] H. Cui, Z. Zhu, Z. Gan, and T. Brogårdh, "Kinematic analysis and error modeling of TAU parallel robot," *Robotics and Computer Integrated Manufacturing*, vol. 21, no. 6, pp. 497–505, 2005.

[5] M. Isaksson, T. Brogårdh, I. Lundberg, and S. Nahavandi, "Improving the Kinematic Performance of the SCARA-Tau PKM," in *IEEE International Conference on Robotics and Automation (ICRA'10)*, Anchorage, AK, USA, 2010, pp. 4683–4690.

[6] T. Brogårdh, S. Hanssen, and G. Hovland, "Application-Oriented Development of Parallel Kinematic Manipulators with Large Workspace," in *2nd International Colloquium of the Collaborative Research Center, 562: Robotic Systems for Handling and Assembly*, Braunschweig, Germany, 2005, pp. 153–170.

[7] M. Isaksson, T. Brogårdh, and S. Nahavandi, "Parallel Manipulators with a Rotation-Symmetric Arm System," *Journal of Mechanical Design*, vol. 134, no. 11, 114503, 2012.

[8] M. Isaksson, "Analysis and Synthesis of Parallel Manipulators with Rotation-Symmetric Arm Systems," Ph.D. dissertation, Deakin University, 2013.

[9] M. Isaksson, T. Brogårdh, M. Watson, S. Nahavandi, and P. Crothers, "The Octahedral Hexarot — A novel 6-DOF parallel manipulator," *Mechanism and Machine Theory*, vol. 55, pp. 91–102, 2012.

[10] C. Gosselin and J. Angeles, "Singularity Analysis of Closed-Loop Kinematic Chains," *IEEE Transactions on Robotics and Automation*, vol. 6, no. 3, pp. 281–290, 1990.